Available online at www.sciencedirect.com
SCIENCE DIRECT®
Biochemical and Biophysical Research Communications 330 (2005) 97–103
BBRC
www.elsevier.com/locate/ybbrc

N-terminal helix reorients in recombinant C-fragment of *Clostridium botulinum* type B

Seetharaman Jayaraman [a], Subramaniam Eswaramoorthy [a], S. Ashraf Ahmed [b], Leonard A. Smith [b], Subramanyam Swaminathan [a,*]

[a] *Biology Department, Brookhaven National Laboratory, Upton, NY 11973, USA*
[b] *Department of Immunology and Molecular Biology, Division of Toxicology, United States Army Medical Research Institute of Infectious Diseases, Fort Detrick, MD 21702, USA*

Received 3 February 2005

Abstract

Botulinum neurotoxins comprise seven distinct serotypes (A–G) produced by *Clostridium botulinum*. The crystal structure of the binding domain of the botulinum neurotoxin type B (BBHc) has been determined to 2 Å resolution. The overall structure of BBHc is well ordered and similar to that of the binding domain of the holotoxin. However, significant structural changes occur at what would be the interface of translocation and binding domains of the holotoxin. The loop 911–924 shows a maximum displacement of 14.8 Å at the farthest point. The N-terminal helix reorients and moves by 19.5 Å from its original position. BBHc is compared with the binding domain of the holotoxin of botulinum type A and B, and the tetanus C-fragment to characterize the heavy chain-carbohydrate interactions. The probable reasons for different binding affinity of botulinum and tetanus toxins are discussed.
Published by Elsevier Inc.

Keywords: *Clostridium botulinum*; Binding domain; X-ray crystallography; Three-dimensional structure; Gangliosides

Botulinum neurotoxin (BoNT) is a member of the clostridial neurotoxin family (CNT), which includes seven botulinum neurotoxins (A to G) and tetanus (TeNT) toxin. CNTs are the most potent toxins having selective high affinity binding to neurons. BoNTs act at the neuromuscular junction causing flaccid paralysis while TeNT acts on peripheral nervous system causing spastic paralysis. These toxins are synthesized as inactive single chain proteins of ~150 kDa and released as di-chains cleaved either by endogenous or exogenous proteases. The di-chain is composed of a heavy chain (100 kDa) and a light chain (50 kDa) associated via both inter-chain interactions and the conserved disulfide bond between heavy and light chains [1,2].

Polysialogangliosides bind CNTs on the C-terminal domain of heavy chain [3]. Many experimental studies have predicted the location, binding specificity, and affinity for ganglioside binding on the C-terminal subdomain of CNTs [4–10]. A double receptor model has been suggested for CNTs, binding to neuronal cells and might involve both the subdomains [11]. Low (K_d in nM range) and high (K_d in sub-nM) affinity receptors for CNTs have been identified and experimental evidences prove that for high affinity binding, both lipid and protein receptors are essential [3]. It has been shown that the C-terminal domain of BoNT and TeNT (TeHc) is necessary and sufficient for binding and internalization of these proteins into neurons [12].

The crystal structures of BoNT/A and B show that the molecules have three distinct structural domains corresponding to three functional domains; (i) the catalytic

* Corresponding author. Fax: +1 631 344 3407.
E-mail address: swami@bnl.gov (S. Swaminathan).

0006-291X/$ - see front matter. Published by Elsevier Inc.
doi:10.1016/j.bbrc.2005.02.123

domain containing Zn-metalloprotease active site; (ii) a translocation domain containing a long loop (residues 481–532), called the belt region that wraps around the catalytic domain; and (iii) a binding domain. The amino acid sequence of the binding domains is well conserved among all clostridial neurotoxins, suggesting that they may have a closely similar structure [13,14]. The crystal structures of the binding domain of TeHc, BoNT/A and B show two distinct subdomains within the binding domain, N- and C-terminal domains [15–17]. The C-terminal β-trefoil domain contains folds related to those present in several other proteins involved in recognition and binding functions, such as various trypsin inhibitors, and the N-terminal domain contains a lentil lectin-like jelly-roll motif [18].

A number of studies have illustrated the importance of the C-terminal region of the β-trefoil domain, however the lectin-like carbohydrate binding N-terminal domain has received less attention. The crystal structures of BoNT/B with doxorubicin and sialyllactose [17] show that both bind at the same site and crystal structures of TeHc with sialic acid, *N*-acetylgalactosamine, GT1b, galactose, disialyllactose, and a tripeptide (YEW) show that they bind in four different sites. Interestingly, all these binding sites are in the C-terminal domain [8,10,19,20]. Though N-terminal domain is similar to lectin carbohydrate binding domain, so far there has been no evidence of sugars binding in this region.

BoNT and TeNT act by blocking neurotransmitter release. Their mechanism of action on target nerve cells consists of binding, internalization, and membrane translocation by heavy chain and enzymatic target cleavage by light chain [1]. Separation of the domains from the holotoxin is expected to result in significant structural changes since the hydrophobic contacts at the interface would be lost [21]. Binding domains of botulinum toxins are being actively pursued as potential vaccine candidates. Since a potential vaccine candidate should evoke the same kind of immune response as the binding domain in the holotoxin, no large structural change should occur. The structural work was undertaken to test whether the structural integrity is maintained when the binding domain is separated from the holotoxin. Here, we report the crystal structure of the binding domain of BoNT/B (BBHc) and compare, with the holotoxin binding domain of BoNT/A and B, and TeHc.

Experimental

BBHc containing residues 853–1290 of *Clostridium botulinum* type B, Danish strain was expressed from a synthetic gene in *Pichia pastoris* and purified as described [22]. The protein in 0.05 M $NaPO_4$ buffer at pH 7.5, with, initial concentration of 0.130 mg/ml was dialyzed against 0.02 M Hepes and 0.1 M NaCl at pH 7.5, for 48 h in four changes at 4 °C. The protein was then concentrated to 6.5 mg/ml. Crystallization screening was carried out with Hampton Crystal Screen, and two or three conditions were selected. The best condition was with ammonium acetate which gave very small crystals and was later successfully replaced by ammonium formate. Sitting drop crystallization was set up with a droplet containing a mixture of 1 μl protein, 1 μl of 60–100 mM ammonium formate, and 1 μl of 30% PEG 6000. Different sugars and additives were tried to improve the quality of the crystal. Addition of 0.3 μl of the additive 2 M non-detergent Sulfo-betaine 201 gave better crystals. The reservoir solution consists of 20% PEG6000 and 0.1 M Hepes at pH 7. Rod-shaped crystals of dimension $0.05 \times 0.06 \times 0.08$ mm appeared after a week and diffracted to 1.9 Å. Crystals are in space group $P2_1$ with cell dimensions $a = 68.66$, $b = 78.81$, $c = 88.72$ Å and $\beta = 103.03°$. Matthews coefficient (V_m) was calculated to be 2.37 $Å^3$/Da based on two molecules per asymmetric unit [23]. The two molecules in the asymmetric unit are related by a twofold at 1/4 along *c*-axis, parallel and halfway between crystallographic twofold screws.

Data were collected at liquid nitrogen temperature at X25 beam line of the NSLS, Brookhaven National Laboratory with Q315 detector. An oscillation range of 1° was used for each data frame with the crystal to detector distance of 280 mm and $\lambda = 1.01$ Å. Data were processed by HKL2000 [24].

The structure was determined by the molecular replacement method using the poly-alanine model of the binding domain of the previously determined BoNT/B structure (PDB id: 1ERW) as the search model [25]. Loops were truncated in the model to avoid model bias. After initial rigid body refinement, side chains were included in the model. The model was refined by slow cool simulated annealing method with CNS and in each step, $2F_{obs} - F_{calc}$ and $F_{obs} - F_{calc}$ maps were calculated to check and improve the model in the density maps using the program O [26,27]. Cycles of rebuilding and refinement were

Table 1
Data reduction and refinement statistics

Space group	$P2_1$
Number of molecules per asymmetric unit	2
Unit cell	$a = 68.66$, $b = 78.81$, $c = 88.72$ Å and $\beta = 103.03°$
Resolution (Å)	2.0
$I/\sigma(I)$	11.0
Redundancy	4.0 (3.2)[a]
No. of unique reflections	59,503 (4723)
Completeness	96 (77)
R_{merge}[b]	0.09 (0.48)
R-factor[c]	0.23
R_{free}[d]	0.28
No. of protein atoms	3564
No. of water molecules	431
Average *B*-factor (Å)	
Protein	32.3
Water molecules	38.1
RMSD	
Bond lengths (Å)	0.01
Bond angles (°)	1.50

[a] Values in parentheses are for the highest resolution shell, 2.07–2.0 Å.

[b] $R_{merge} = \sum|I_i - \langle I \rangle|/\sum|I_i|$, where I_i is the intensity of the *i*th measurement, and $\langle I \rangle$ is the mean intensity for that reflection.

[c] *R*-factor $= \sum|F_{obs} - F_{calc}|/\sum|F_{obs}|$, where F_{calc} and F_{obs} are the calculated and observed structure factor amplitudes, respectively.

[d] R_{free} = as for R_{cryst}, but for 10.0% of the total reflections chosen at random and omitted from refinement.

continued until the convergence of *R*-factor and *R*-free. A total of 430 water molecules were located from the difference Fourier maps and were included in subsequent rounds of refinement. The model is complete except that 1150–1156 loop region is disordered. Data reduction and refinement statistics are listed in Table 1 (PDB id: 1Z0H).

Results and discussion

BBHc structure

The structure of the BBHc has been determined to 2.0 Å resolution. The molecule has maximum dimension of approximately $33 \times 42 \times 80$ Å^3 and has 438 residues from Asn853 to Glu1290. The molecule comprises two similar sized subdomains (C- and N-terminal domains) which have limited surface interactions with each other. The tertiary structure suggests that the two domains fold independently. The N-terminal domain has 16 β-strands (which includes a set of seven-stranded antiparallel β-sheets) and three α-helices, and the C-terminal domain has 16 β-strands and one α-helix (Fig. 1). The overall structure of BBHC is well ordered and globally similar to that of the binding domain of holotoxin structure, except for the orientation of two loops located on the surface of the molecule and the N-terminal helix [17]. Analysis of the model using PROCHECK shows that all non-proline and non-glycine residues are found in the most favored or additionally allowed region of the Ramachandran plot [28].

Fig. 1. Ribbon diagram showing the tertiary structure of the binding domain of BBHc.

Table 2
Binding domain, translocation domain interactions in holotoxin BoNT/B

Binding domain	Translocation domain	Distance (Å)
Tyr 855 OH	Lys 784 NZ	2.94
Asn 866 ND2	Asp 615 OD2	2.96
Arg 868 NH1	Ile 613 O	3.31
Arg 868 NH2	Asp 615 OD2	3.30
	Ile 613 O	3.43
Lys 870 NZ	Asn 640 OD1	3.28
	Lys 785 NZ	2.68
Tyr 880 OH	Lys 784 NZ	3.19
Asn 915 OD1	Glu 792 N	3.51

Separation of BD

The binding domain and the rest of the holotoxin are linked through the N-terminal α-helix of the binding domain. In the holotoxin structure, the binding domain is tilted away from the central translocation domain and makes minimal contact with it. The two domains interact via nine hydrogen bonds (Table 2). There are 13 other possible hydrophilic contacts within 4.8 Å as calculated by the program CONTACT from the CCP4 suite of programs (Collaborative Computational Project, No. 4, 1994). Water molecules in the interface play an important role in binding these domains [17]. In addition, numerous hydrophobic contacts are observed between the two domains involving the N-terminal helix and the loop at the interface (aa 911–924). The separation of binding domain causes the loss of these interactions resulting in major loop movements.

BBHc and BoNT/B

Comparison of the isolated binding domain and the binding domain of holotoxin was carried out to evaluate structural changes. The superposition of BBHc on BoNT/B holotoxin binding domain (Fig. 2) shows that the N-terminal helix and loop regions on the surface of the molecule do not superimpose, particularly the loop at translocation and binding domain interface. Overall, one loop in the N-terminal domain and two loops in the C-terminal domain show significant displacements. (i) In the holotoxin, the N-terminal helix (aa 846–856) of binding domain is close and almost orthogonal to long helices in the translocation domain and makes extensive contacts with the translocation domain helices (Table 2). The N-terminal helix bridges the two domains. After the domain separation, it loses all its interactions and moves 19.5 Å away from its position changing its orientation. Its orientation is similar to

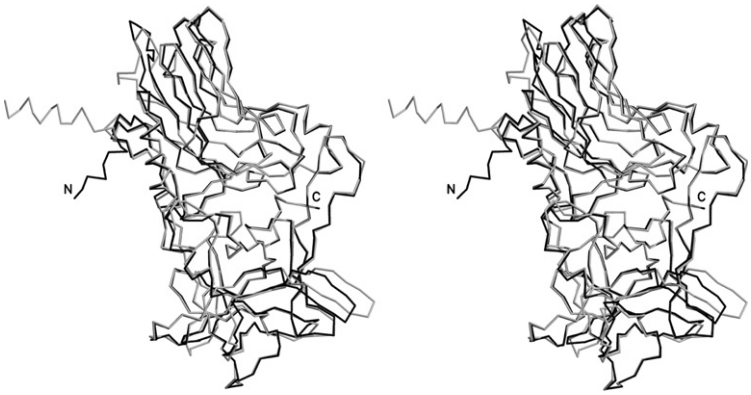

Fig. 2. Stereo view of superposition of isolated binding domain with the binding domain of the holotoxin. Black-isolated binding domain and gray-holotoxin.

those of the corresponding helices in the binding domain of BoNT/A and TeHc. However, BoNT/A is a holotoxin whereas TeHc is binding domain only. (ii) The loop (aa 911–924) at the interface of translocation and binding domain which makes direct hydrogen bonds with the translocation domain is displaced by 14.7 Å in the absence of these interactions. The buried hydrophobic residues at this region are exposed in BBHc. The solvent accessibility of the loop in the absence of translocation domain increases. (iii) One of the loops in the C-terminal region (aa 1245–1250) moves away from its position by 7.5 Å. This region binds sialyllactose and doxorubicin in the cleft between His1240 and Trp1261 [8,17]. Though the extended loop shows a displacement, the binding pocket which is at the beginning of the loop region maintains its shape and size. This loop movement may not affect any binding in this region. The binding site comparison shows a general widening of the ligand binding cleft at the extended binding site region that can facilitate the binding.

As the binding domain shows significant changes, its counterpart at translocation domain is expected to show similar changes particularly at the interface region on separating it from holotoxin. The separation of catalytic domain of BoNT/B showed similar rearrangement of the loops in the active site exposing the active site for binding [29]. Such changes are also observed in BoNT/E and TeNT (KN Rao, unpublished) catalytic domains [30].

Comparison with BoNT/A and TeNT binding domain

The binding domains of BoNT/B, BoNT/A, and TeNT have 438, 430, and 441 residues, respectively. Fig. 3A shows the superposition of the Cα atoms of BBHc (green), binding domain of BoNT/A (blue) and TeHc (red). The rms deviation between BBHc and BoNT/A is 1.4 Å for 349 Cα atoms, and between BBHc and TeHc is 1.3 Å for 346 Cα atoms. The three models provide general information on the heavy chain-carbohydrate interactions. The superposition shows that the core β-strand regions superimpose fairly well whereas loop regions do not.

Hc–carbohydrate interaction

There are two BoNT/B complex structures and six TeHc complex structures available for comparison, to understand the Hc–carbohydrate interaction of the binding domain. BoNT/B and TeNT have a common binding site, Site-1 (Fig. 3A). This site in BoNT/B binds sialyllactose and doxorubicin (His1240 and Tyr1262 region), and in TeNT binds lactose and part of GT1b (Gal-GalNac) (His1271 and Tyr1290 region) [10,19]. The binding pocket has the same size and shape in both molecules as this region is structurally and sequentially well conserved. Various biochemical studies indicated that this region of β-trefoil subdomain of clostridial neurotoxins was involved in ganglioside binding. Site-directed mutagenesis showed that Tyr1290 plays a key role in binding of ganglioside in TeNT [6]. This tyrosine appears to be conserved throughout CNTs: Tyr1290 in TeNT, Tyr1266 in BoNT/A, and Tyr1262 in BoNT/B. Ganglioside-photoaffinity ligand study implicated that His1293 of this region in TeNT is important for ganglioside binding [31]. Gln1269 in BoNT/A and Glu1265 in BoNT/B can play a similar role as His1293 in TeNT with a similar stacking of the side chain of Trp1289, which is used to maintain the binding pocket in proper shape for the binding to occur. Fluorescence experiments suggested that Trp1265 must be part of ganglioside binding site in BoNT/A [32]. Trp1261 in BoNT/B was shown to be involved in binding sialyllactose in this region [17]. As BoNT/A has the same sequence and structural motif, it is also expected to bind ganglioside in this region. This site is a conserved site and represents the general binding pocket of clostridial neurotoxins. As there is no antidote available for botulinum at present,

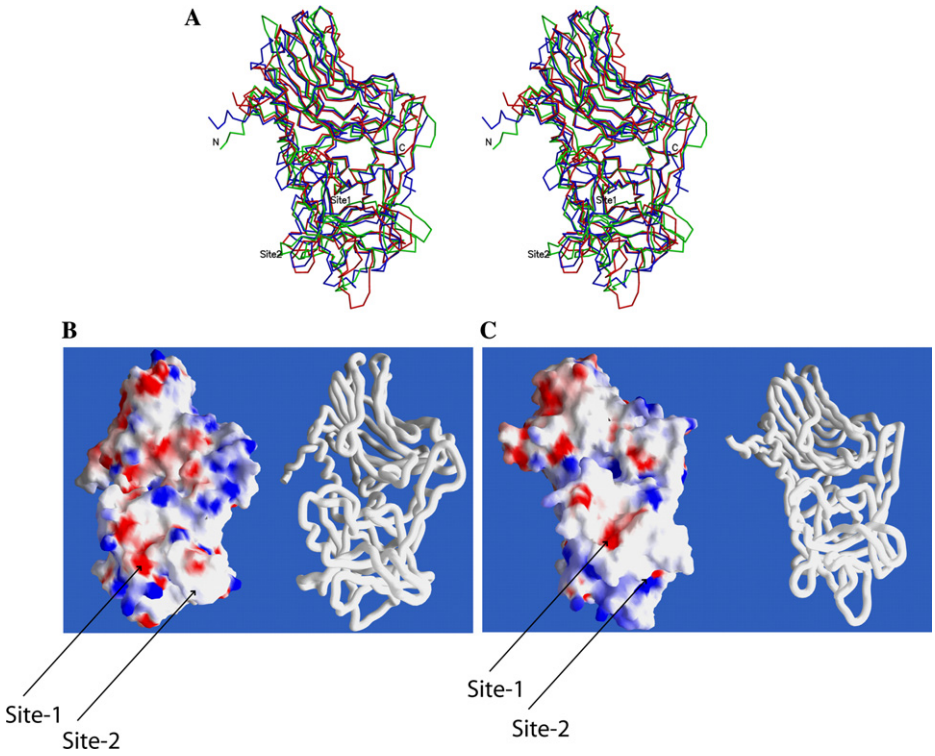

Fig. 3. (A) Stereo view of superposition of the Cα atoms of BBHc (green), TeHc (red), and binding domains of BoNT/A (blue). (B) Electrostatic potential of the recombinant binding domain of BoNT/B. Blue and red represent the positive and negative electrostatic potentials, respectively. Adjacent figure shows the worm representation of the molecule. Site-1 and Site-2 are marked. (C) A similar representation for TeHc.

this site is a potential target for development of therapeutics.

The other important site, Site-2 (Fig. 3A), the region around 1114–1147 of TeHc, binds sialic acid, disialyllactose, YEW, and Gal-NAc part of GT1b [10,19,20]. In this region, there is no structural evidence of any binding in BoNT/A and B. A comparison with BoNT/A and B shows that the length and orientation of the loops forming the binding site are different. The key residues Asp1214, Asn1216, Asp1147, and Tyr1229 that interact with bound ligands in TeHc are on the loop region and are not conserved in BoNT/A and B. This is the unique and most common sugar-binding site for TeNT but differs structurally and sequentially from BoNT/A and B.

The electrostatic potential surface shows the similarity and dissimilarity among the binding sites in the binding domain of BoNT/B and TeHc (Fig. 3B) [33]. The lactose and Gal-GalNAc binding site (Site-2) of TeHc is formed by the side chains of Asp1214, Asn1216, Arg1226, and Tyr1229; this site in TeHC is formed by charged residues while in BoNT/B they are mostly hydrophobic (This region in BoNT/B is made of side chains of Phe1193, Val1117, Leu1194, Val1227, Pro1116, Phe1242, and Phe1203). The electrostatic potential surface at this site is positive in TeHc and neutral in BoNT/B. The shape and electrostatic potential properties of lactose binding site (Site-1) of TeHc (formed by residues Asn1220, Asp1222, Thr1270, Ser1287, Trp1289, Tyr1290, and Gly1300) and sialyllactose-binding site of BoNT/B (formed by residues His1240, Try1262, Glu1189, and Glu1188) appear to be similar. The bottom of the pocket shows a highly hydrophilic patch in TeHc and BoNT/B formed by the structurally equivalent residues. In TeHc, this includes the side chain oxygen of residues Asp1222, Ser1287, and Tyr1290, and the main chain carbonyl oxygen of Thr1270. These residues play a key role in binding the galactose unit of ganglioside [10]. The corresponding residues, Ser1287, Tyr1262 in BoNT/B, play a key role in binding sialyllactose in this region [17]. Tyr1262 of BoNT/B makes two strong hydrogen bonds with the silalic acid part of sialyllactose agreeing with the results of Sutton et al. [6] indicating that Tyr1262 plays an important role in ganglioside binding.

Conclusion

The structure of BBHc shows that the separation of the binding domain from the rest of holotoxin results in large displacements of the loop and the N-terminal helix connecting the translocation and binding domains. This is probably the reason why the C-fragment is a very poor competitor of the toxin for receptor binding. There are no significant changes in the sialyllactose-

binding site between BBHc and BoNT/B-binding domain. Comparison of electrostatic charge distribution of BBHc and TeHc at the binding sites explains the probable reason for the difference in binding affinity between the two.

Acknowledgments

The research was supported by the U.S Army Medical Research Acquisition Activity (Award No. DAMD17-02-2-0011) under DOE Prime Contract No. DE-AC02-98CH10886 with Brookhaven National Laboratory. We thank Dr. D. Kumaran for helpful discussions and Dr. M. Becker for providing beam time at the National Synchrotron Light Source, Brookhaven National Laboratory.

References

[1] G. Schiavo, M. Matteoli, C. Montecucco, Neurotoxins affecting neuroexocytosis, Physiol. Rev. 80 (2000) 717–766.
[2] A. de-Paiva, B. Poulain, G.W. Lawrence, C.C. Shone, L. Tauc, J.O. Dolly, A role for the interchain disulfide or its participating thiols in the internalization of botulinum neurotoxin A revealed by a toxin derivative that binds to ecto-acceptors and inhibits transmitter release intracellularly, J. Biol. Chem. 268 (1993) 20838–20844.
[3] J.L. Halpern, E.A. Neale, Neurospecific binding, internalization, and retrograde axonal transport, Curr. Top. Microbiol. Immunol. 195 (1995) 221–241.
[4] H.A. Louch, E.S. Buczko, M.A. Woody, R.M. Venable, W.F. Vann, Identification of a binding site for ganglioside on the receptor binding domain of tetanus toxin, Biochemistry 41 (2002) 13644–13652.
[5] A. Rummel, S. Bade, J. Alves, H. Bigalke, T. Binz, Two carbohydrate binding sites in the H(CC)-domain of tetanus neurotoxin are required for toxicity, J. Mol. Biol. 326 (2003) 835–847.
[6] J.M. Sutton, O. Chow-Worn, L. Spaven, N.J. Silman, B. Hallis, C.C. Shone, Tyrosine-1290 of tetanus neurotoxin plays a key role in its binding to gangliosides and functional binding to neurones, FEBS Lett. 493 (2001) 45–49.
[7] J.L. Halpern, A. Loftus, Characterization of the receptor-binding domain of tetanus toxin, Nature 268 (1993) 11188–11192.
[8] S. Eswaramoorthy, D. Kumaran, S. Swaminathan, Crystallographic evidence for doxorubicin binding to the receptor-binding site in *Clostridium botulinum* neurotoxin B, Acta Cryst. D57 (2001) 1743–1746.
[9] C. Fotinou, P. Emsley, I. Black, H. Ando, H. Ishida, M. Kiso, K.A. Sinha, N.F. Fairweather, N.W. Isaacs, The crystal structure of tetanus toxin Hc fragment complexed with a synthetic Gt1b analogue suggests cross-linking between ganglioside receptors and the toxin, J. Biol. Chem. 276 (2001) 32274–32281.
[10] P. Emsley, C. Fotinou, I. Black, N.F. Fairweather, I.G. Charles, C. Watts, E. Hewitt, N.W. Isaacs, The structures of the H(C) fragment of tetanus toxin with carbohydrate subunit complexes provide insight into ganglioside binding, J. Biol. Chem. 275 (2000) 8889–8894.
[11] C. Montecucco, How do tetanus and botulinum toxins bind to neuronal membranes? Trends Biochem. Sci. 11 (1986) 314–317.
[12] G. Lalli, J. Herreros, S.L. Osbrone, C. Montecucco, O. Rossetto, G. Schiavo, Functional characterisation of tetanus and botulinum neurotoxins binding domains, J. Cell Sci. 112 (1999) 2715–2724.
[13] N.P. Minton, Molecular genetics of clostridial neurotoxins, Curr. Top. Microbiol. Immunol. 195 (1995) 161–194.
[14] F.J. Lebeda, M.A. Olson, Structural predictions of the channel-forming region of botulinum neurotoxin heavy chain, Toxicon 33 (1995) 559–567.
[15] T.C. Umland, L.M. Wingert, S. Swaminathan, W.F. Furey, J.J. Schmidt, M. Sax, Structure of the receptor binding fragment H_c of tetanus neurotoxin, Nat. Struct. Biol. 4 (1997) 788–792.
[16] D.B. Lacy, W. Tepp, A.C. Cohen, B.R. DasGupta, R.C. Stevens, Crystal structure of botulinum neurotoxin type A and implications for toxicity, Nat. Struct. Biol. 5 (1998) 898–902.
[17] S. Swaminathan, S. Eswaramoorthy, Structural analysis of the catalytic and binding sites of *Clostridium botulinum* neurotoxin B, Nat. Struct. Biol. 7 (2000) 693–699.
[18] J.S. Richardson, The anatomy and taxonomy of protein structure, Adv. Protein Chem. 34 (1981) 167–339.
[19] C. Fotinou, P. Emsley, I. Black, H. Ando, H. Ishida, M. Kiso, K.A. Sinha, N.F. Fairweather, N.W. Isaacs, The crystal structure of tetanus toxin Hc fragment complexed with a synthetic GT1b analogue suggests cross-linking between ganglioside receptors and the toxin, J. Biol. Chem. 276 (2001) 32274–32281.
[20] J. Seetharaman, S. Eswaramoorthy, D. Kumaran, S. Swaminathan, A common binding site for disialyllactose and a tripeptide in the C-fragment of tetanus neurotoxin, Proteins (2005) in press.
[21] D.B. Lacy, R.C. Stevens, Sequence homology and structural analysis of clostridial neurotoxins, J. Mol. Biol. 291 (1999) 1091–1104.
[22] K.J. Potter, M.A. Bevins, E.V. Vassilieva, V.R. Chiruvolu, T. Smith, L.A. Smith, M.M. Meagher, Production and purification of the heavy-chain fragment C of botulinum neurotoxin, serotype B, expressed in the methylotrophic yeast *Pichia pastoris*, Protein Expr. Purif. 13 (1998) 357–365.
[23] B.W. Matthews, Solvent content of protein crystals, J. Mol. Biol. 33 (1968) 491–497.
[24] Z. Otwinowski, W. Minor, Processing of X-ray diffraction data collected in oscillation mode, Methods Enzymol. 276 (1997) 307–326.
[25] J. Navaza, P. Saludjian, AMoRe: an automated molecular replacement program package, Methods Enzymol. 276 (1997) 581–594.
[26] A.T. Brunger, P.D. Adams, G.M. Clore, W.L. Delano, P. Gros, R.W. Grosse-Kunstleve, J.S. Jiang, J. Kuszewski, M. Nilges, N.S. Pannu, R.J. Read, L.M. Rice, T. Somonsom, G.L. Warren, Crystallography and NMR system: a new software suite for macromolecular structure determination, Acta Crystallogr. D54 (1998) 905–921.
[27] T.A. Jones, J. Zou, S. Cowtan, M. Kjeldgaard, Improved methods in building protein models in electron density map and the location of errors in these models, Acta Crystallogr. A47 (1991) 110–119.
[28] R.A. Laskowski, M.W. MacArthur, D.S. Moss, J.M. Thornton, PROCHECK: a program to check the stereochemical quality for assessing the accuracy of protein structures, J. Appl. Crystallogr. 26 (1993) 283–291.
[29] M.A. Hanson, R.C. Stevens, Cocrystal structure of synaptobrevin-ll bound to botulinum neurotoxin type B at 2.0 Å resolution, Nat. Struct. Biol. 7 (2000) 687–692.
[30] R. Agarwal, S. Eswaramoorthy, D. Kumaran, T. Binz, S. Swaminathan, Structural analysis of botulinum neurotoxin type E catalytic domain and its mutant Glu212->Gln reveals the pivotal role of the Glu212 carboxylate in the catalytic pathway, Biochemistry 43 (2004) 6637–6644.

[31] R.S. Shapiro, C.D. Specht, B.E. Collins, A.S. Woods, R.J. Cotter, R.L. Schnaar, Identification of a ganglioside recognition domain of tetanus toxin using a novel ganglioside photoaffinity ligand, J. Biol. Chem. 272 (1997) 30380–30386.
[32] Y. Kamata, M. Yoshimoto, S. Kozaki, Interaction between botulinum neurotoxin type A and ganglioside: ganglioside inactivates the neurotoxin and quenches its tryptophan fluorescence, Toxicon 35 (1997) 1337–1340.
[33] A. Nicholls, K.A. Sharp, B. Honig, Protein folding and association: insights from the interfacial and thermodynamic properties of hydrocarbons, Proteins: Struct. Funct. Genet. 11 (1991) 281–296.